

Test of exotic scalar and tensor interactions in K_{e3} decay using stopped positive kaons

A.S. Levchenko^a, A.N. Khotiantsev^a, A.P. Ivashkin^a, M. Abe^b,
M.A. Aliev^a, V.V. Anisimovsky^a, M. Aoki^c, I. Arai^b,
Y. Asano^b, T. Baker^{c,d}, M. Blecher^e, P. Depommier^f,
M. Hasinoff^g, K. Horie^b, H.C. Huangⁱ, Y. Igarashi^c,
T. Ikeda^j, J. Imazato^c, M.M. Khabibullin^a, Y.G. Kudenko^a,
Y. Kuno^{c,h}, L.S. Lee^k, G.Y. Lim^{k,c}, J.A. Macdonald^l,
D.R. Marlow^m, C.R. Mindas^m, O.V. Mineev^a, C. Rangacharyulu^d,
S. Shimizu^b, Y.-M. Shin^d, A. Suzuki^b, A. Watanabe^b,
N.V. Yershov^a, T. Yokoi^c

(E246 KEK-PS COLLABORATION)

^aInstitute for Nuclear Research of RAS, Moscow 117312, Russia;

^bUniversity of Tsukuba, 305-0006, Japan;

^cKEK, 305-0801, Japan;

^dUniversity of Saskatchewan, S7N 0W0, Canada;

^eVirginia Polytechnic Institute and State University, USA;

^fUniversity of Montreal, H3C 3J7, Canada;

^gUniversity of British Columbia, Vancouver, V6T 1Z1 Canada;

^hOsaka University, 560-0043, Japan;

ⁱNational Taiwan University, Taipei, Taiwan;

^jInstitute of Physical and Chemical Research, Hirosewa 2-1, Japan;

^kKorea University, Seoul 136-701, Korea;

^lTRIUMF, V6T 2A3, Canada;

^mPrinceton University, NJ 08544, USA.

Abstract

The form factors of the decay $K^+ \rightarrow \pi^0 e^+ \nu$ (K_{e3}) have been determined from the comparison of the experimental and Monte Carlo Dalitz distributions containing about 10^5 K_{e3} events. The following values of the parameters were obtained: $\lambda_+ = 0.0278 \pm 0.0017(stat) \pm 0.0015(syst)$, $f_S/f_+(0) = 0.0040 \pm 0.0160(stat) \pm 0.0067(syst)$ and $f_T/f_+(0) = 0.019 \pm 0.080(stat) \pm 0.038(syst)$. Both scalar f_S and tensor f_T form factors are consistent with the Standard Model predictions of zero values.

1 Introduction

The most general Lorentz invariant form of the matrix element of K_{e3} decay can be written as [1,2]:

$$\begin{aligned} M \propto & f_+(q^2)(P_K + P_{\pi^0})^\lambda \bar{u}_e \gamma_\lambda (1 - \gamma_5) u_\nu \\ & + f_-(q^2) m_l \bar{u}_e (1 - \gamma_5) u_\nu + 2m_K f_S \bar{u}_e (1 - \gamma_5) u_\nu \\ & + (2f_T/m_K)(P_K)^\lambda (P_{\pi^0})^\mu \bar{u}_e \sigma_{\lambda\mu} (1 - \gamma_5) u_\nu, \end{aligned} \quad (1)$$

where $f_\pm(q^2)$, f_S and f_T are the vector, scalar and tensor form-factors, P_K and P_π are four-momenta of the K^+ and π^0 . The vector form-factors $f_\pm(q^2)$ are assumed to be linearly dependent on the momentum transfer squared $q^2 = (P_K - P_\pi)^2$ and they can be represented by the equation $f_\pm(q^2) = f_\pm(0)(1 \pm \lambda_\pm(q^2/m_{\pi^0}^2))$. Because of the small mass of the positron the part of the matrix element that depends on $f_-(q^2)$ is negligible and there are just three free parameters of the theory: λ_+ , f_S and f_T . Within the Standard Model (SM), due to W -boson exchange, no terms other than those of a pure vector nature are expected. A possible contribution to f_S and f_T from electroweak radiative corrections is negligibly small and, therefore, nonzero values of f_S and f_T would signal new physics beyond the SM. Actually, such deviations from zero for these form factors were measured in [1,3], but were not confirmed in a recent experiment [4], where f_S and f_T were measured with sensitivity similar to Refs. [1,3].

In this paper, we present results of a reanalysis of K_{e3} data taken with the E246 detector at the KEK 12-GeV proton synchrotron. The first result obtained using this data set was published in [4].

2 Experiment

The experiment was performed using the set-up constructed to search for T-violation in $K^+ \rightarrow \pi^0 \mu^+ \nu$ decay. The experimental arrangement is shown in Fig. 1, and is described in detail elsewhere [5–8]. Kaons with $P_{K^+} = 660$ MeV/ c are identified by a Cherenkov counter, slowed in a BeO degrader and then stopped in a target array of 256 scintillating fibers located at the center of a 12-sector superconducting toroidal spectrometer. Charged particles from kaon decays in the target were tracked by means of multiwire proportional chambers at the entrance (C2) and exit (C3 and C4) of each magnet sector, along with the target and a scintillation ring hodoscope around the target. The momentum resolution of $\sigma_p = 2.6$ MeV/ c at $p = 205$ MeV/ c was obtained using mono-energetic products from the two-body decay $K^+ \rightarrow \pi^+ \pi^0$.

The energies and angles of the photons from π^0 decays are measured by a CsI(Tl) photon detector consisting of 768 modules [6]. The photon detector covers a solid angle of 3π steradians, with openings for the beam entry and exit and 12 holes for charged particles to pass into the magnet gaps. The photon energy was obtained by summing the cluster energy distributed among several crystals surrounding a central

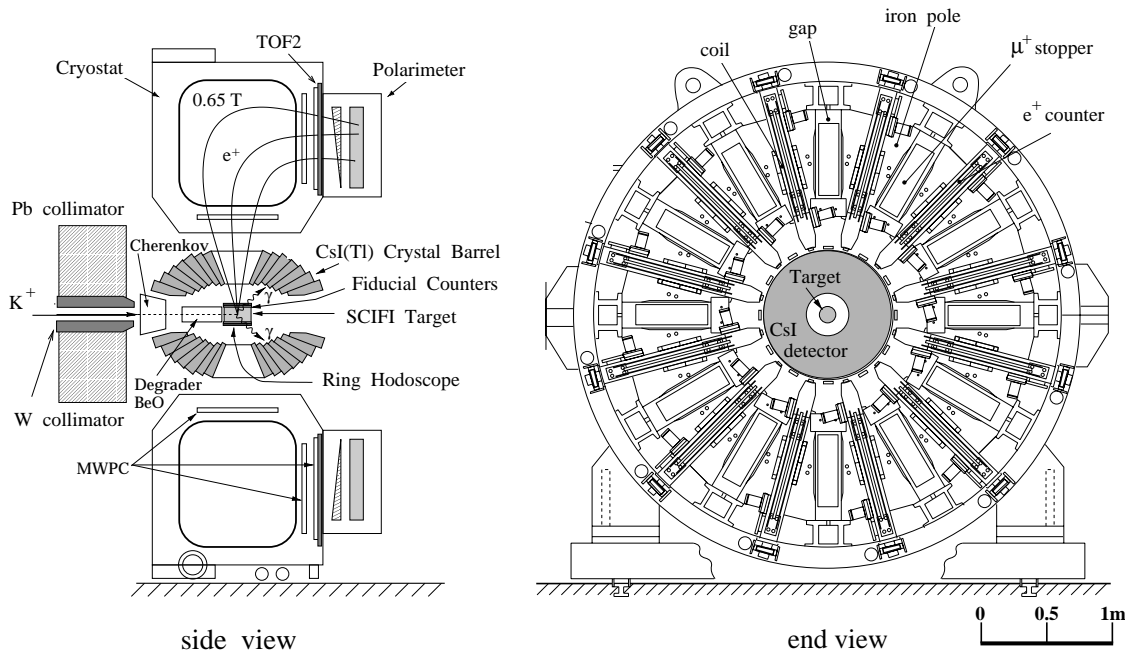


Figure 1: The layout of the E246 set-up

crystal. The position of the photon cluster is determined using an energy-weighted “center-of-gravity” method. To suppress accidental background from the beam, timing information from each crystal was used. A time resolution of 3.8 nsec (σ) for the wide photon energy range of 10–220 MeV was achieved. The energy resolution was obtained to be $\sigma_{E_\gamma}/E_\gamma \simeq 3.0\%$ at $E_\gamma = 150$ MeV. The invariant mass resolution of $\sigma_{\gamma\gamma} = 7.5$ MeV/ c^2 at $M_{\gamma\gamma} = 133.1$ MeV/ c^2 , and angular resolution of $\sigma_\theta = 2.4^\circ$ were obtained in the experiment [6, 9].

The study of the K_{e3} decay required a trigger condition different from that of the main experiment. The following trigger was used to accumulate K_{e3} events

$$C_K \times Fid_i \times TOF2_i \times 2\gamma \times GapVeto. \quad (2)$$

The Cherenkov condition C_K ensures that the beam particle is a K^+ . The coincidence between C_K , delayed by 2 nsec, and the fiducial counters (Fid_i) for the charged particles eliminates the triggers due to decays in flight. The time of flight signal from the corresponding gap ($TOF2_i$) completes the charged particle trigger condition. The trigger also required two hits in the CsI (2γ). The requirement $GapVeto$ eliminates events where the charged particle may have lost energy in the CsI crystals around the i^{th} hole.

The K_{e3} data were collected for two spectrometer field settings, B=0.65 and B=0.9 Tesla.

3 Analysis

K_{e3} events were selected using the following requirements. A clean hit pattern in the target and a delayed decay at least 2 nsec after the K^+ arrival time measured by Cherenkov counter suppressed the K^+ decays-in-flight. Cuts on the charged-particle momentum, $p < 190$ MeV/ c , and the opening angle between e^+ and π^0 , $\theta_{e^+\pi^0} < 170^\circ$, effectively removed the $K_{\pi 2}$ events. π^+ decays-in-flight were rejected by a cut on the track reconstruction $\chi^2 < 14$. The photon conversion events were suppressed by requiring single hits in the ring and fiducial counters and a single track in the target. Events with more than two hits in the electromagnetic calorimeter were rejected. The cut on the invariant mass was $75 < M_{\gamma\gamma} < 140$ MeV/ c^2 . The main criterion separating K_{e3} positrons from $K_{\mu 3}$ muons was derived from the time-of-flight (TOF) measurement between the fiducial counters and scintillating counters (TOF2) located at the exit of each spectrometer gap (see Fig. 1). The mass squared of the charged particle was determined as

$$M^2 = P^2((L/\tau \cdot c)^2 - 1), \quad (3)$$

where L and τ are the length and time of flight of the charged particle between fiducial and TOF2 counters, and c is the speed of light in vacuum. The TOF resolution is $\sigma_{TOF} = 300$ ps, and the mass squared spectrum is shown in Fig. 2. To separate positrons from muons, a cut on the mass squared $-4500 < M_{TOF}^2 < 4500$ MeV $^2/c^4$ was chosen.

Compared to the analysis of [4], improvements in reconstruction of the charged particle track were made. In the new analysis, information about the kaon stopping position from the target (x, y) and ring counter (z) was included in the momentum reconstruction routine. The reconstruction of the π^0 kinematics was also improved by using tighter time windows in the CsI and improved calibration. The Monte Carlo routines properly included the correct kaon stopping distribution in the target and the electromagnetic shower leakage effects in the CsI. This allowed us to use all CsI crystals for reconstruction of the π^0 , while in Ref. [4] events were rejected where either photon hit a crystal adjacent to the 12 charged-particle holes. Overall optimization resulted in approximately a factor of four increase in acceptance. For 0.65-T magnetic field we extracted 102k good K_{e3} events with background contamination of 0.21% from $K_{\mu 3}$ and 0.34% from $K_{\pi 2}$ decays.

The distributions of the $e^+ - \pi^0$ opening angle and the opening angle between photons from $\pi^0 \rightarrow \gamma\gamma$ for K_{e3} decay is shown in Fig. 3. Energy spectra of the K_{e3} decay are shown in Fig. 4.

The extraction method for the parameters is based on comparison of the experimental and Monte Carlo Dalitz distributions. If one allows for the existence of the exotic interactions, the Dalitz plot density is given by [10]:

$$\rho(E_e, E_\pi) = f_+^2(q^2)(A + B\xi(q^2) + C\xi^2(q^2)) \quad (4)$$

where

$$A = m_K(2E_e E_\nu - m_K E'_\pi) + m_e^2(E'_\pi/4 - E_\nu)$$

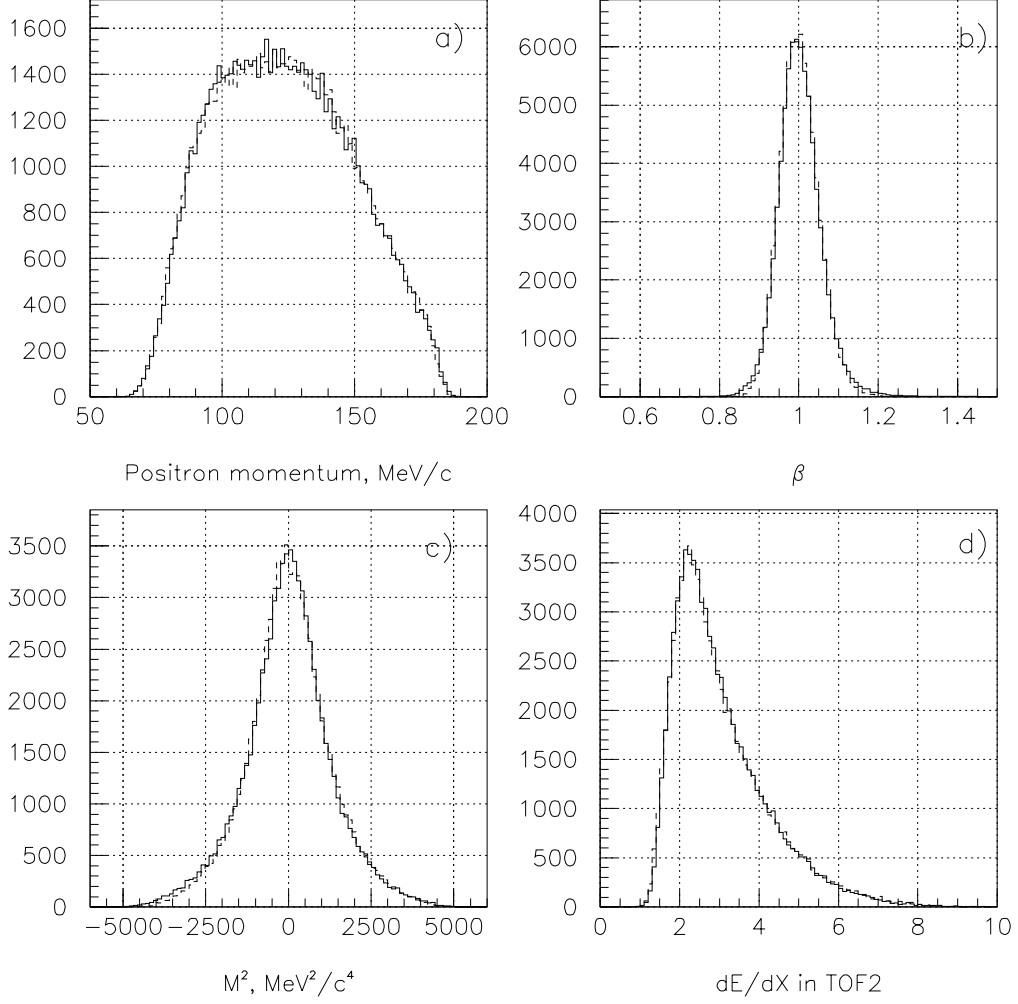


Figure 2: (a) Momentum spectrum of e^+ from K_{e3} decay; (b) β spectra of e^+ ($\beta = \frac{L}{\tau \cdot c}$); (c) reconstructed TOF mass squared of e^+ ; (d) energy deposit of e^+ in TOF2 counter. Solid line corresponds to experimental and dashed line to GEANT-simulated events.

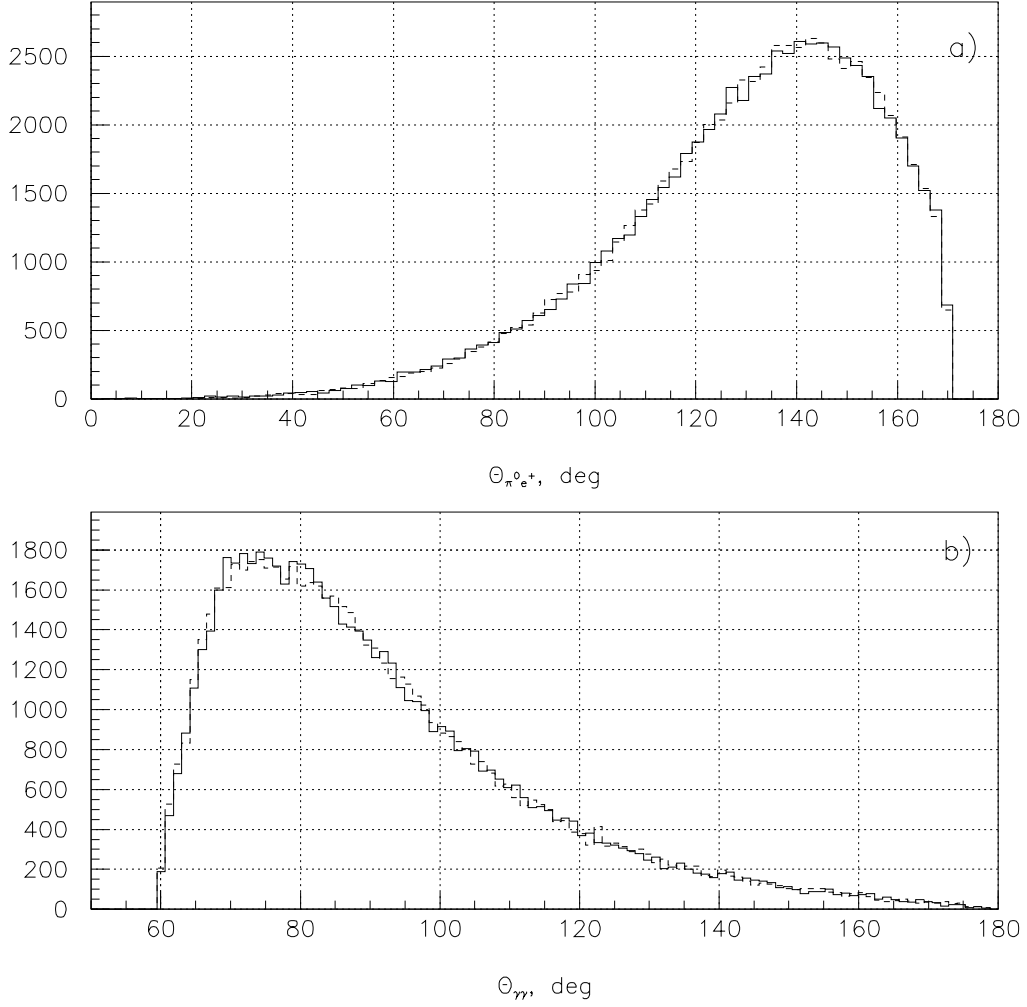


Figure 3: K_{e3} decays: a) angle between e^+ and π^0 ; b) angle between photons $\theta_{\gamma\gamma}$. Solid line - experiment, dashed line - Monte Carlo.

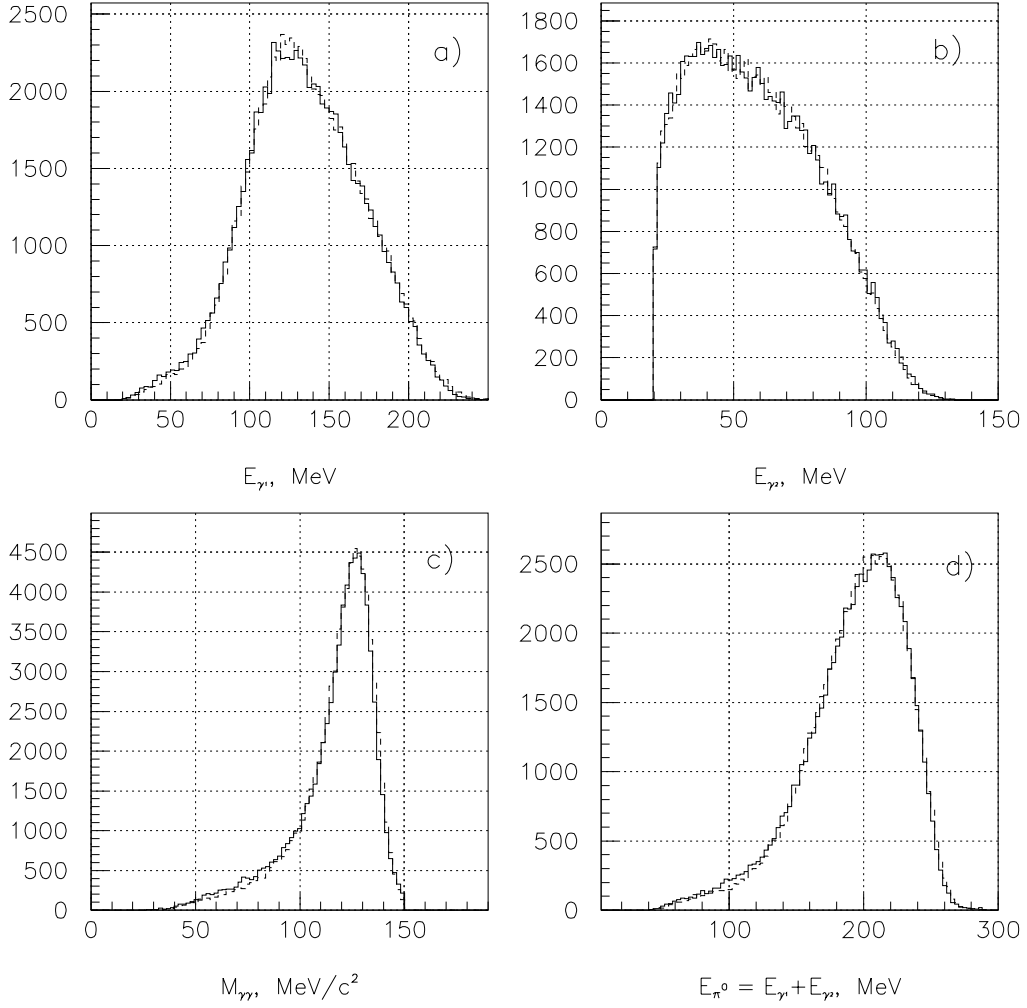


Figure 4: K_{e3} decays: a) energy of γ_1 ($E_{\gamma_1} > E_{\gamma_2}$); b) energy of γ_2 ; c) invariant mass $M_{\gamma\gamma}$; d) energy of π^0 ($E_{\pi^0} = E_{\gamma_1} + E_{\gamma_2}$). Solid line - experiment, dashed line - Monte Carlo.

$$\begin{aligned}
B &= (m_e^2)(E_\nu - E'_\pi/2) \\
C &= (m_e^2)E'_\pi/4 \\
E'_\pi &= (m_K^2 + m_\pi^2 - m_e^2)/(2m_K) - E_\pi \\
\xi(q^2) &= \frac{(2m_K/m_e)R_S + (m_e/m_K + 2(E_\nu - E_e)/m_e)R_T}{(1 + (m_e/m_K)R_T)} \\
R_S &= f_S/f_+ \quad \quad R_T = f_T/f_+
\end{aligned}$$

The parameters of the decay can be extracted by selecting the minimum of the χ^2 variable defined as

$$\chi^2 = 2 \cdot \sum_{i=1}^n (N_i^{MC} - N_i^{exp}) + N_i^{exp} \cdot \log\left(\frac{N_i^{exp}}{N_i^{MC}}\right), \quad (5)$$

where n is the number of bins over the Dalitz plot, N_i^{MC} the number of Monte Carlo events in each bin, and N_i^{exp} the number of experimental events in each bin.

Within the Standard Model the only parameter to be obtained is λ_+ . It can be extracted in a model-independent way from the q^2 dependence of f_+ . Using eq. 4, $\sqrt{\rho(E_e, E_\pi)} \propto f_+ = f_+(0)(1 + \lambda_+ q^2/m_{\pi^0}^2)$, and, therefore, λ_+ can be extracted from the ratio

$$(N_{exp}/N_{mc}(\lambda_+ = 0))^{1/2} = (1 + \lambda_+ q^2/m_{\pi^0}^2). \quad (6)$$

The q^2 dependence of this ratio shown in Fig. 5 allows us to determine the value $\lambda_+ = 0.0278 \pm 0.0016(stat)$.

For extraction of all three parameters λ_+ , f_S and f_T , the Dalitz distribution fit was performed using the P_{e+} , $\theta_{\pi^0 e+}$ variables. The angle between the pion and positron, $\theta_{\pi^0 e+}$, was preferred instead of pion energy E_{π^0} in order to reduce a systematic error related to the energy leakage in the electromagnetic calorimeter. The bin sizes chosen were $\Delta P_{e+} = 3.125$ MeV/c and $\Delta \theta_{e+\pi^0} = 4.2^\circ$. Radiative corrections to the Dalitz plot were taken into account according to Ginsberg [11]. The χ^2 between experimental and Monte Carlo Dalitz distributions was minimized by a program based on MINUIT [12]. The values obtained for λ_+ , and the scalar and tensor form factors are

$$\begin{aligned}
\lambda_+ &= 0.0278 \pm 0.0017(stat) \\
f_S/f_+(0) &= 0.004 \pm 0.016(stat) \\
f_T/f_+(0) &= 0.019 \pm 0.080(stat).
\end{aligned} \quad (7)$$

Since our analysis relies on the proper detector responses used by the Monte Carlo simulation, comparisons and checks were made wherever possible. For example, to check the values obtained and to see possible unknown systematic effects, a similar analysis of the scatter plot $\theta_{\gamma\gamma}$ vs. P_{e+} was also performed. From this approach it was found that $\lambda_+ = 0.0281 \pm 0.0017(stat)$, $f_S/f_+(0) = 0.001 \pm 0.018(stat)$, and

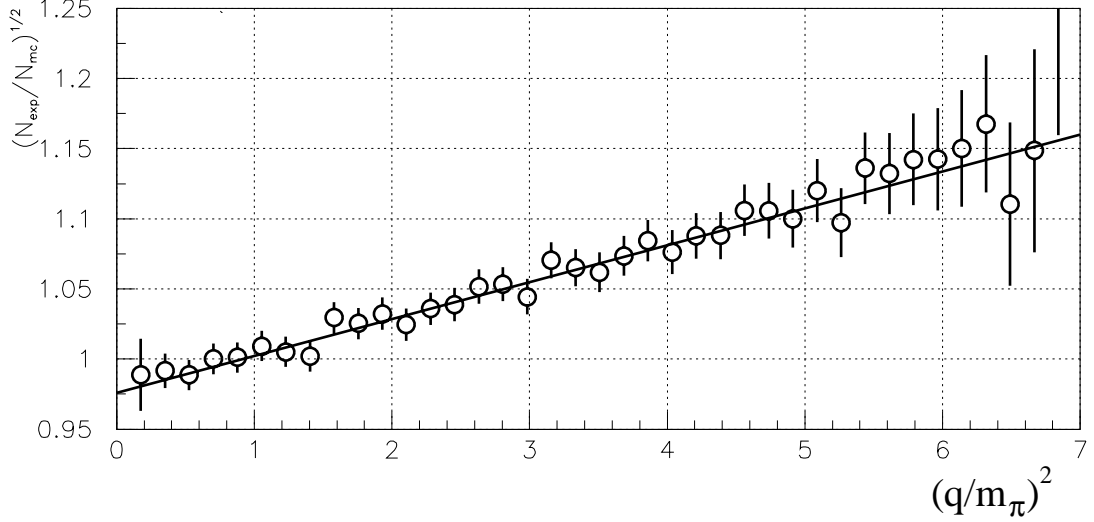


Figure 5: The q^2 dependence of the ratio N_{exp}/N_{mc} . The straight line shows a linear fit with $\lambda_+ = 0.0278$.

$f_T/f_+(0) = 0.007 \pm 0.100(stat)$. No significant variations of the λ_+ value were seen, and values of the form factors were consistent with zero within a 1σ uncertainty.

The main sources of systematic errors were related to detector inefficiencies, misalignments of the detector elements, background contamination, and uncertainties connected to the Monte Carlo simulation. All these sources were studied and the estimations of the systematic errors are presented in Table 1.

4 Result

The result presented here is based on about 10^5 good K_{e3} events. We have obtained

$$\begin{aligned}\lambda_+ &= 0.0278 \pm 0.0017(stat) \pm 0.0015(syst) \\ f_S &= 0.0040 \pm 0.0160(stat) \pm 0.0067(syst) \\ f_T &= 0.019 \pm 0.080(stat) \pm 0.038(syst).\end{aligned}\tag{8}$$

Using only one data set at $B=0.65$ T, we have improved statistical errors by a factor of 1.5 and systematic errors for λ_+ , f_S and f_T were reduced by the factors 2.0, 2.1, and 2.4, respectively, compared to our previous result [4]. This result is in agreement with the Standard Model prediction and there is no evidence for a deviation from zero for the values of scalar and tensor form factors. We expect to further improve our accuracy after completing the analysis of the K_{e3} data accumulated at $B=0.9$ T.

Table 1: Systematic errors.

| Source | λ_+ | f_S | f_T |
|---------------------------------------------|-------------|--------|--------|
| MWPC's misalignment | 0.0006 | 0.0010 | 0.0022 |
| MWPC's spatial resolution | 0.0002 | 0.0010 | 0.0010 |
| e^+ identification | 0.0007 | 0.0022 | 0.0004 |
| Bremsstrahlung | 0.0010 | 0.0015 | 0.0280 |
| χ^2 cut point | 0.0001 | 0.0010 | 0.0018 |
| CsI barrel misalignment | 0.0005 | 0.0042 | 0.0240 |
| E_γ and $M_{\gamma\gamma}$ cut point | 0.0003 | 0.0020 | 0.0027 |
| $\gamma \rightarrow e^+e^-$ conversion | 0.0001 | 0.0018 | 0.0100 |
| Pile-up in the CsI | 0.0004 | 0.0013 | 0.0015 |
| Total | 0.0015 | 0.0067 | 0.0380 |

References

- [1] H.J. Steiner et.al., Phys. Lett. **B36** (1971) 521.
- [2] Particle Data Group, D.E. Groom et al., Eur. Phys. J. **C15** (2000) 1.
- [3] S.A. Akimenko et al., Phys. Lett. **B259** (1991) 225.
- [4] S. Shimizu et al., Phys. Lett. **B495** (2000) 33.
- [5] M. Abe et al., Phys. Rev. Lett. **83** (1999) 4253.
- [6] D.V. Dementyev et al. Nucl. Instr. Meth. **A440** (2000) 151.
- [7] A.P. Ivashkin et al., Nucl. Instr. Meth. **A394** (1997) 321.
- [8] M.P. Grigorev et al., Instrum. Exp. Tech. **41** (1998) 803 [Prib. Tekh. Eksp. N6 (1998) 65].
- [9] M.M. Khabibullin et al., Instrum. Exp. Tech. **43** (2000) 589 [Prib. Tekh. Eksp. N5 (2000) 9].
- [10] H. Braun et al., Nucl. Phys. **B89** (1975) 210.
- [11] E.S. Ginsberg, Phys. Rev. **162** (1967) 1570.
- [12] F. James, MINUIT Reference Manual, CERN Geneva, 1994.